Proc. Natl. Acad. Sci. USA
Vol. 92, pp. 12046–12049, December 1995
Neurobiology

Three distinct structural environments of a transmembrane domain in the inwardly rectifying potassium channel ROMK1 defined by perturbation

SENYON CHOE*, CHARLES F. STEVENS*†, AND JANE M. SULLIVAN*

*Structural Biology and Molecular Neurobiology Laboratories, and †Howard Hughes Medical Institute, The Salk Institute, La Jolla, CA 92037

Contributed by Charles F. Stevens, September 7, 1995

ABSTRACT **To probe the protein environment of an ion channel, we have perturbed the structure of a transmembrane domain by substituting side chains with those of two different sizes by using site-specific mutagenesis. We have used Trp and Ala as a high- and a low-impact perturbation probe, respectively, to replace each of 18 consecutive residues within the putative second transmembrane segment, M2, of an inwardly rectifying potassium channel, ROMK1. Our rationale is that a change in the channel function as a consequence of these mutations at a particular position will reflect the structural environment of the altered side chain. Each position can then be assigned to one of three classes of environments, as graded by different levels of perturbation: very tolerant (channel functions with both Trp and Ala substitutions), tolerant (function preserved with Ala but not with Trp substitution), and intolerant (either Ala or Trp substitution destroys function). We identify the very tolerant environment as being lipid-facing, tolerant as protein-interior-facing, and intolerant as pore-facing. We observe a strikingly ordered pattern of perturbation of all three environmental classes. This result indicates that M2 is a straight α-helix.**

The activity of ion channels in excitable cells forms the physical basis for neuronal function (1). Despite a wide variety of ion selectivity and modes of regulation, many ion channels appear to share a similar structural architecture (2, 3). Voltage-gated potassium channels are tetrameric assemblies of homo- or heteromeric subunits (4–6), each consisting of six putative transmembrane helices (S1–S6) with a pore-lining P region between the fifth (S5) and the sixth (S6) helix (3, 7, 8). Other ion channels, such as sodium or calcium channels, are assembled as a single polypeptide chain containing four homologous repeats, each of which resembles the subunit of a potassium channel (2, 9–11).

We chose to study the structure of an inwardly rectifying potassium channel because of its apparently simple architecture. From the amino acid sequence of an inwardly rectifying potassium channel, ROMK1 (12), deduced from a cDNA recently cloned from mammalian kidney, it was proposed that each subunit consists of two transmembrane segments, M1 and M2, each including about 21 hydrophobic residues, and a connecting loop H5 between them that contains the P region. M1 and M2 of inwardly rectifying channels correspond to S5 and S6 of the canonical structural motif of voltage-gated potassium, sodium, and calcium channels. The P region is believed to form a hairpin-like turn conformation within the membrane (7, 8, 13, 14) and is primarily responsible for ion selectivity. Thus the M1, M2, and P-region segments of the ROMK1 channel are viewed as the minimum and sufficient structural elements necessary for forming a protein ion channel (12, 15–18).

The publication costs of this article were defrayed in part by page charge payment. This article must therefore be hereby marked "*advertisement*" in accordance with 18 U.S.C. §1734 solely to indicate this fact.

In the absence of detailed structural information, we have reasoned that if the M1 and M2 transmembrane segments are packed around the pore-lining P region, then the protein environment of amino acid side chains projecting from M1 and M2 can be segregated into three classes: lipid-facing, protein-interior-facing, and pore-facing (Fig. 1*A*). These environmental milieu are expected to tolerate structural perturbation introduced by site-specific mutagenesis to different extents. Using two hydrophobic amino acids, Trp and Ala, as perturbation probes, we have formulated the following three criteria in judging the effects of mutational perturbation (Table 1). (*i*) If a mutation to either Ala or Trp preserves channel function, the residue is likely to face the lipid environment. The lipid-exposed exterior surface of the channel would be topologically equivalent to a water-exposed surface of globular proteins, and Trp represents a high-impact perturbation probe because of the large atomic volume of its side chain. The atomic volume of side chains of Ala and Trp are 29 and 168 Å^3, respectively. The numbers of nonhydrogen atoms of the side chains of Ala and Trp are 1 and 11, respectively (21). (*ii*) If a mutation to Trp eliminates channel function but one to Ala does not, the residue is likely to face the protein interior, where a minor change to Ala might be tolerated but the larger Trp side chain could not be accommodated (22–25). Ala represents a low-impact perturbation probe because the geometry of its side chain is common to all amino acids except Gly. (*iii*) If the side chain of the residue is directly facing the hydrophilic channel lining, mutation to either Trp or Ala is likely to eliminate channel function since the pore structure is sensitive to any small structural modifications. Despite the empirical nature of our classification criteria, the data on mutants at 18 consecutive positions within the M2 segment show a remarkable orderliness in the perturbation pattern.

MATERIALS AND METHODS

Mutagenesis of ROMK1. ROMK1 mutants were generated by the PCR-based overlap-extension method of site-directed mutagenesis and were verified by sequencing (26).

Measurement of Channel Activity. *Xenopus* oocytes were injected with up to 5 ng of RNA transcribed *in vitro* by T7 RNA polymerase according to the Ambion (Austin, TX) mMessage mMachine protocol. Two-electrode voltage-clamp recordings were made 1–7 days after RNA injection. Oocytes were continuously superfused with recording solution containing 96 mM KCl, 5 mM Hepes, 1 mM $MgCl_2$, and 0.3 mM $CaCl_2$ (pH 7.6). Current–voltage (*I–V*) relations were generated by ramping the membrane potential from −150 mV to +60 mV over 8.5 sec in the presence and absence of 5 mM barium (a ROMK1 channel blocker) (12) and then by subtracting the *I–V* curve generated in the presence of barium from that observed in the absence of barium. The barium-sensitive potassium current of uninjected oocytes was typically less than 25 nA.

Abbreviation: *I–V*, current–voltage.

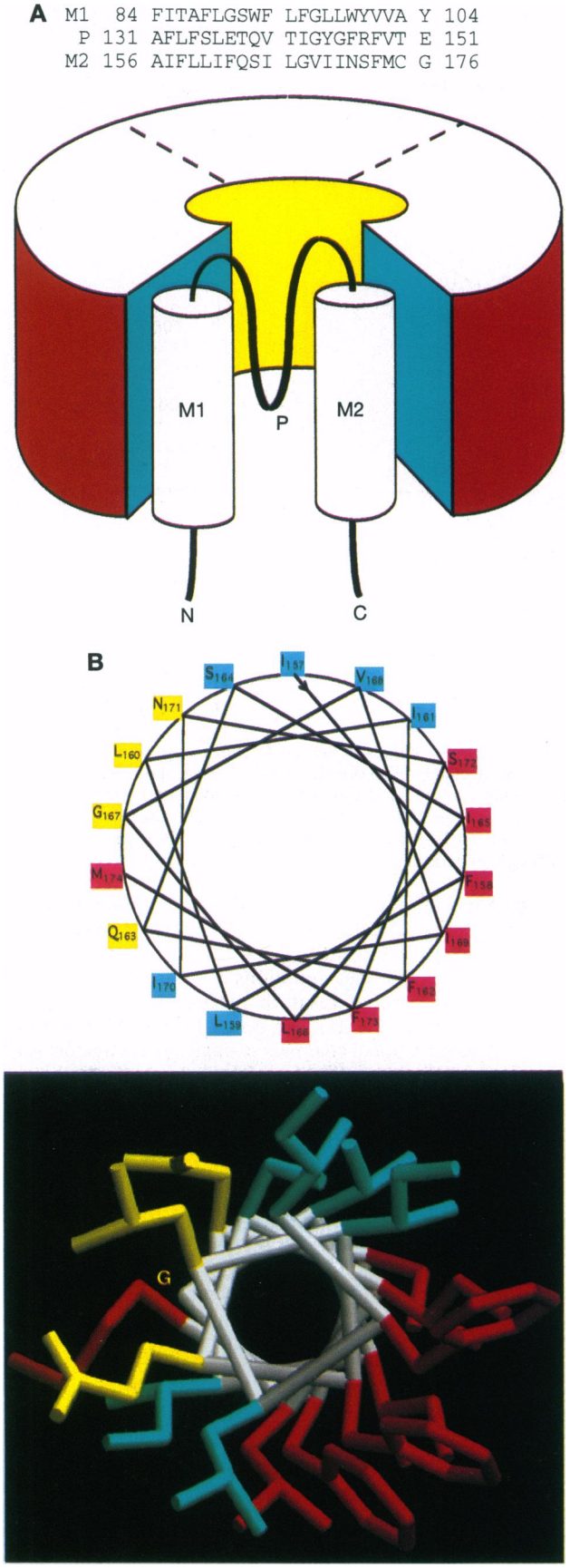

FIG. 1. (*A*) Schematic drawing of a channel. (*Upper*) Amino acid sequences of M1, P-region, and M2 segments of ROMK1 (12). (*Lower*) The drawing is a conceptual representation emphasizing the following points: (*i*) ROMK1 is a tetramer with four subunits related by fourfold rotational symmetry around a central pore, and (*ii*) each subunit consists of M1, M2, and a pore-lining P region. There are three classes of protein environments for these structural elements: lipid-facing channel exterior (red), protein-interior-facing (blue), and pore-facing (yellow). These definitions of environmental classes are independent of the relative disposition of M1, M2, and the P region. The extracellular side of the membrane is upward. (*B*) (*Upper*) Helical wheel diagram generated with a pitch of 3.6 residues per turn. (*Lower*) Lipid-facing (red), protein-interior-facing (blue), and pore-facing (yellow) side chains are shown with the α-helical backbone (white). The canonical backbone coordinates for the helix were generated with the program MIDAS (19), and the side-chain atoms were modeled with the program O (20). G represents the position of Gly-167, which has no side-chain atoms.

Table 1. Summary of classification criteria

Functional environment	Tolerated substitution(s)	Structural environment
Very tolerant	Both Trp and Ala	Lipid-facing channel exterior
Tolerant	Ala but not Trp	Protein interior
Intolerant	Neither Ala nor Trp	Channel pore

Mutant channels were classified as nonfunctional if the barium-sensitive potassium current of oocytes injected with 5 ng of mutant RNA was $\leq$25 nA. The barium-sensitive potassium current of oocytes expressing functional channels was typically greater than 1 μA when 5 ng of RNA was injected.

RESULTS AND DISCUSSION

Table 2 summarizes the results from 32 mutations introduced in M2 of ROMK1. Based on electrophysiological measurements from oocytes injected with RNA of each mutant (Fig. 2), our criteria for classifying the protein environment assign each residue to one of three environmental classes. These results are shown in a helical wheel diagram, in which the three classes are represented by the side chains in three colors (Fig. 1*B*). It is evident that the three classes are clustered when mapped onto an α-helix and their relative positions are in accord with each other.

Side chains in the very tolerant environment (seven lipid-facing residues), colored in red, are all clustered in one area with an angular spread of about 140°, consistent with the model that M2 is a straight helix with these residues exposed to the membrane lipid. Met-174 in this class is an exception, presumably because it lies close to the end of the M2 helix.

Side chains in the intolerant environment (four pore-facing residues), colored in yellow, are all clustered on the side opposite from the lipid-facing residues. Among the four putative pore-facing residues (Leu-160, Gln-163, Gly-167, and Asn-171), position 171 has been implicated as a pore-lining residue (27, 28). The Asn-171 $\rightarrow$ Asp substitution in ROMK1 alters its weak rectification property to that of IRK (a strong inwardly rectifying potassium channel), in which Asp is found at the equivalent position (15), by providing a Mg^{2+} binding site. The idea of Mg^{2+} having direct access to the binding site inside the channel pore is consistent with our model.

Because Gly-167 is unique in having no side-chain atoms that can directly face the pore lining, we have assigned Gly-167 in the pore-facing side according to the following supposition. Based on the result from the Gly-167 $\rightarrow$ Trp mutant, we can first conclude that it is not in the lipid-facing environment. However, Gly-167 $\rightarrow$ Trp could have been nonfunctional because Trp disrupts a unique and essential geometrical flexibility of the M2's peptide backbone atoms provided by Gly (e.g., positive phi and psi angles due to its intrinsic nonchirality). If this were the case, mutation to any other amino acid at this position would disrupt such a conformation regardless of its protein environment. This possibility can be eliminated because mutation to Ala at position 167 retains channel

Table 2. Summary of mutation data

ROMK1 residue	Mutation		Environmental class
	Ala	Trp	
Ile-157	F	NF	Interior
Phe-158	—	F	Lipid
Leu-159	F	NF	Interior
Leu-160	NF	NF	Pore
Ile-161	F	NF	Interior
Phe-162	—	F	Lipid
Gln-163	NF	NF	Pore
Ser-164	F	NF	Interior
Ile-165	F	F	Lipid
Leu-166	F	F	Lipid
Gly-167	F	NF	Pore*
Val-168	F	NF	Interior
Ile-169	F	F	Lipid
Ile-170	F	NF	Interior
Asn-171	NF	NF	Pore
Ser-172	F	F	Lipid
Phe-173	—	F	Lipid
Met-174	—	F	Lipid

F and NF refer to functional and nonfunctional channels, respectively. Mutants showing barium-sensitive current no larger than that of uninjected oocytes were assigned to NF (see Fig. 2). Lipid, interior, and pore refer to lipid-facing exterior, protein-interior-facing, and channel-pore-facing environments. —, Mutant was not made because it is not needed for the classification purpose.
*See text for explanation.

function, indicating that Gly-167 does not cause a kink in the helix and validating our interpretation that position 167 is not lipid-facing. Thus, position 167 belongs to either the pore-facing or protein-interior-facing environments. A straightforward interpretation of these data (functional Gly-167 → Ala and nonfunctional Gly-167 → Trp) according to our classification criteria would be that position 167 is in the protein-interior-facing environment, if it were a non-Gly residue. Instead, we have concluded that Gly-167 is in the pore-facing environment, on the basis of the helical perturbation pattern of all other positions and because the structural role of Gly's "nonexisting" side-chain atoms is effectively as if they were buried in a protein-interior-facing environment.

Side chains in the tolerant environment (six protein-interior-facing residues), colored in blue, are clustered in two regions flanking each side of the lipid-facing region of the M2 helix, sandwiched between the pore-facing and the lipid-facing sides. Homotetrameric assemblies of ROMK1 subunits are probably arranged with a fourfold rotational symmetry around the channel pore, as seen in the electron microscopic image of the voltage-gated Shaker potassium channel (29). Therefore, the finding that the protein-interior-facing residues are clustered in two separate regions suggests that the two protein-interior-facing sides of M2 interface with two different regions: presumably, one within the same subunit and the other within a neighboring subunit.

Supporting our classification criteria is the observation that those positions that are intolerant of the low-impact probe are always intolerant of the high-impact probe, and those tolerant of the high-impact probe are also tolerant of the low-impact probe. An opposite case where a position tolerated a high-impact probe but did not tolerate a low-impact probe (i.e., a Trp-insensitive and Ala-sensitive mutant) was never observed. Additionally, there was no apparent correlation between the consequence of mutation and other physical characteristics such as the size and hydrophobicity of the side chain at the position where a mutation was introduced. For instance, there are three Leu residues in M2, and mutations to Ala or Trp at Leu-159, Leu-160, and Leu-166 resulted in all three possible combinations of nonfunctional and functional channels. These

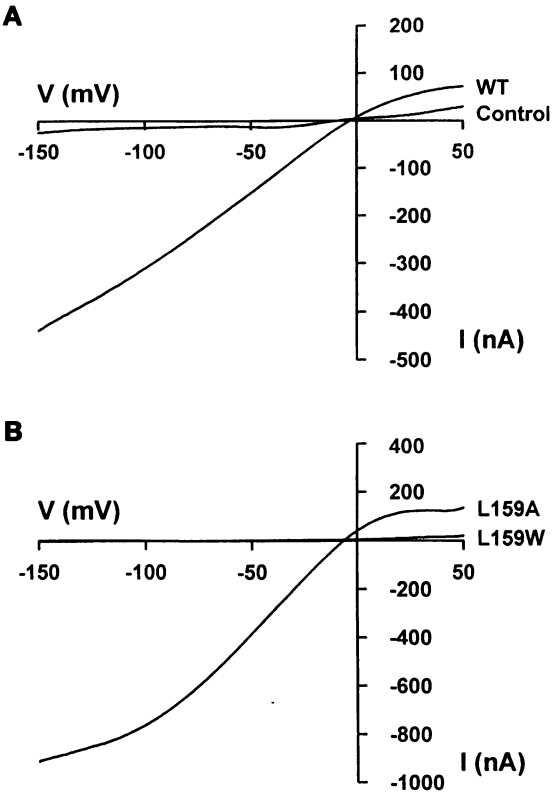

FIG. 2. (*A*) *I–V* curves of an oocyte expressing wild-type ROMK1 and an uninjected control oocyte. (*B*) *I–V* curves of oocytes expressing a functional mutant, L159A, and a nonfunctional mutant, L159W. The *I–V* curves of functional channels were generated from oocytes injected with 0.05–0.5 ng of RNA to avoid saturation of the amplifier at strongly hyperpolarized membrane potentials.

findings support our assumption that the consequence of mutation mainly reflects the level of structural tolerance to perturbation within the channel.

While it is possible that mutations at some positions of the oocyte-expressed protein result in inefficient transport to the membrane surface (30, 31), the periodic clustering of functional and nonfunctional channels strongly argues against such a possibility. This internal self-consistency among the helical perturbation patterns of the three environmental classes is the strongest evidence that the periodic pattern in perturbation accurately reflects the helical nature of the M2 structure.

The relatively subtle structural change introduced by a single-point mutation leading to a dramatic change in channel function may be the result of a 4-fold amplification in homotetramers to a level at which the mutational effect can be observed. For this reason, our strategy of differential perturbation by a combination of small and large hydrophobic probes, Ala and Trp, might be particularly effective in probing other homomultimeric ion channels.

Transmembrane domains of membrane proteins determined at atomic resolution have invariably shown ordered secondary structural motifs and relatively simple orientation with respect to the membrane (32–40). Such a structural constraint is believed to be due to a low dielectric constant within the membrane (41, 42). Although the notion of differential perturbation by size is not directly applicable to probing the structural environments of globular proteins, it will be generally applicable to probing transmembrane domains of membrane proteins.

We thank Quynh-Chi Phan for preparing the oocytes and Christopher Boyer for sequencing the ROMK1 mutants. We acknowledge support from the Lucille P. Markey Charitable Trust, Joseph Drown

Foundation, George Hoag Family Foundation, Mary Hillman Jennings Foundation, J. W. Kieckhefer Foundation, Esther A. S. and Joseph Klingenstein Fund, and Wynn Foundation. C.F.S. is a Howard Hughes Medical Institute Investigator.

1. Hille, B. (1992) *Ionic Channels of Excitable Membranes* (Sinauer, Sunderland, MD), 2nd Ed.
2. Catterall, W. A. (1988) *Science* **242,** 50–61.
3. Miller, C. (1991) *Science* **252,** 1092–1096.
4. Papazian, D. M., Schwarz, T. L., Tempel, B. L., Jan, Y. N. & Yan, L. Y. (1987) *Science* **237,** 749–753.
5. MacKinnon, R. (1991) *Nature (London)* **350,** 232–235.
6. Li, M., Jan, Y. N. & Yan, L. Y. (1992) *Science* **257,** 1225–1230.
7. MacKinnon, R. & Yellen, G. (1990) *Science* **250,** 276–279.
8. Yellen, G., Jurman, M. E., Abramson, T. & MacKinnon, R. (1991) *Science* **251,** 939–942.
9. Noda, M., Shimizu, S., Tanabe, T., Takai, T., Kayano, T., Ikeda, T., Takahashi, H., Nakayama, H., Kanaoka, Y., Minamino, N., Kangawa, K., Matsuo, H., Raftery, M. A., Hirose, T., Inayama, S., Hayashida, H., Miyata, T. & Numa, S. (1984) *Nature (London)* **312,** 121–127.
10. Noda, M., Ikeda, T., Suzuki, H., Takeshima, H., Takahashi, T., Kuno, M. & Numa, S. (1990) *Nature (London)* **322,** 826–828.
11. Tanabe, T., Takeshima, H., Mikami, A., Flockerzi, V., Takahashi, H., Kangawa, K., Kojima, M., Matsuo, H., Hirose, T. & Numa, S. (1987) *Nature (London)* **328,** 313–318.
12. Ho, K., Nichols, C. G., Lederer, W. J., Lytton, J., Vassilev, P. M., Kanazirska, M. V. & Hebert, S. C. (1993) *Nature (London)* **362,** 31–38.
13. Lü, Q. & Miller, C. (1995) *Science* **268,** 304–307.
14. Pascual, J. M., Shieh, C., Kirsch, G. E. & Brown, A. M. (1995) *Neuron* **14,** 1055–1063.
15. Kubo, Y., Baldwin, T. J., Jan, Y. N. & Jan, L. Y. (1993) *Nature (London)* **362,** 127–133.
16. Jan, L. Y. & Jan, Y. N. (1994) *Nature (London)* **371,** 119–122.
17. Dascal,,N., Schreibmayer, W., Lim, N. F., Wang, W., Chavkin, C., DiMagno, L., Labarca, C., Kieffer, B. L., Gaveriaux-Ruff, C., Trollinger, D., Lester, H. A. & Davidson, N. (1993) *Proc. Natl. Acad. Sci. USA* **90,** 10235–10239.
18. Doupnik, C. A., Davidson, N. & Lester, H. A. (1995) *Curr. Opin. Neurobiol.* **5,** 268–277.
19. Ferrin, T. E., Huang, C. C., Jarvis, L. E. & Langridge, R. (1988) *J. Mol. Graphics* **6,** 13–27.
20. Jones, T. A., Zou, J.-Y., Cowan, S. W., Kjeldgaard, M. (1991) *Acta Crystallogr. A* **47,** 110–119.
21. Singh, J. & Thornton, J. M. (1992) *Atlas of Protein Side-Chain Interactions* (IRL, Oxford).
22. Blundell, T. L., Sibanda, B. L., Sternberg, M. J. & Thornton, J. M. (1987) *Nature (London)* **326,** 347–352.
23. Baldwin, E. P., Hajiseyedjavadi, O., Baase, W. A. & Matthews, B. W. (1993) *Science* **262,** 1715–1718.
24. Lim, W. A., Farruggio, D. C. & Sauer, R. T. (1992) *Biochemistry* **31,** 4324–4333.
25. Clackson, T. & Wells, J. A. (1995) *Science* **267,** 383–386.
26. Ho, S. N., Hunt, H. D., Horton, R. M., Pullen, J. K. & Pease, L. R. (1989) *Gene* **77,** 51–59.
27. Lu, Z. & MacKinnon, R. (1994) *Nature (London)* **371,** 243–246.
28. Wible, B. A., Taglialatela, M., Ficker, E. & Brown, A. M. (1994) *Nature (London)* **371,** 246–249.
29. Li, M., Unwin, N., Stauffer, K. A., Jan, L. Y. & Jan, Y. N. (1994) *Curr. Biol.* **4,** 110–115.
30. Cheng, S. H., Gregory, R. J., Marshall, J., Paul, S., Souza, D. W., White, G. A., O'Riordan, C. R. & Smith, A. E. (1990) *Cell* **63,** 827–834.
31. Lukacs, G. L., Chang, X. B., Bear, C., Kartner, N., Mohamed, A., Riordan, J. R. & Grinstein, S. (1993) *J. Biol. Chem.* **268,** 21592–21598.
32. Deisenhofer, J., Epp, O., Miki, K., Huber, R. & Michel, H. (1985) *Nature (London)* **318,** 618–624.
33. Weiss, M. S., Abele, U., Weckesser, J., Welte, W., Schiltz, E. & Schulz, G. E. (1991) *Science* **254,** 1627–1630.
34. Cowan, S. W., Schirmer, T., Rummel, G., Steiert, M., Ghosh, R., Pauptit, R. A., Jansonius, J. N. & Rosenbusch, J. P. (1992) *Nature (London)* **358,** 727–733.
35. Kreusch, A., Neubuser, A., Schiltz, E., Weckesser, J. & Schulz, G. E. (1994) *Protein Sci.* **3,** 58–63.
36. Kühlbrandt, W., Wang, D. N. & Fujiyoshi, Y. (1994) *Nature (London)* **367,** 614–621.
37. Schirmer, T., Keller, T. A., Wang, Y. F. & Rosenbusch, J. P. (1995) *Science* **267,** 512–514.
38. McDermott, G., Prince, S. M., Freer, A. A., Hawthornthwaite-Lawless, A. M., Papiz, M. Z., Cogdell, R. J. & Isaacs, N. W. (1995) *Nature (London)* **374,** 517–521.
39. Tshkihara, T., Aoyama, H., Yanashita, E., Tomizaki, T., Yamaguchi, H., Shinzawa-Itoh, K., Nakashima, R., Yaono, R. & Yoshikawa, S. (1995) *Science* **269,** 1069–1074.
40. Iwata, S., Ostermeier, C., Ludwig, B. & Michel, H. (1995) *Nature (London)* **376,** 660–669.
41. Cramer, W. A., Engelman, D. M., Von Heijne, G. & Rees, D. C. (1992) *FASEB J.* **6,** 3397–3402.
42. Cowan, S. W. & Rosenbusch, J. P. (1994) *Science* **264,** 914–916.